Journal of Computational Applied Mechanics 2023, 54 (1): 36-48

DOI: 10.22059/JCAMECH.2023.351326.773

RESEARCH PAPER

Convective MHD Jeffrey Fluid Flow Due to Vertical Plates with Pulsed Fluid Suction:A Numerical Study

G. Murali [a, *], NVN. Babu [b]

[a] *Department of Mathematics, Sreenidhi University, Hyderabad, India.*
[b] *Department of Engineering Science, Sanjivani College of Engineering, Kopargaon, India.*

Abstract

This main script is concerned with the study of MHD natural convective non-newtonian Jeffrey fluid flow with Hall current, heat source and variable suction towards a vertical plate. By using similarity variables the governing non-linear partial differential equations are transformed into linear partial differential equations and these equations together with associated boundary conditions are solved numerically by using versatile, extensively validated, variational finite element method. The sway of key parameters, on hydrodynamic and thermal boundary layers are examined in detail and the results are shown graphically. A comparative study is also provided in sense of limiting cases for verification and an excellent agreement is found. This model has important applications in industrial thermal management, geological flows in the earth mantle, MHD pumps, accelerators and flow meters, geothermal reservoirs and underground energy transport, etc

Keywords: Hall Current; Heat Source; MHD; Jeffrey Fluid; FEM.

1. Main text

Non-Newtonian fluids have gained interest because of their numerous technological applications, including manufacturing of plastic sheets, performance of lubricants, and movement of biological fluids. In particular, the boundary layer flow of an incompressible non-Newtonian fluid over a stretching sheet has several industrial applications, for few examples of industrial applications for boundary layer flow of an incompressible non-Newtonian fluid across a stretching sheet include the extrusion of a polymer sheet from a dye, drawing of plastic films, oil recovery, food processing, and paper manufacture. Jeffrey fluid is a subclass of fluids, namely, has attracted a lot of attention in the last few years. Because its constitutive equation can be reduced to that of the Newtonian model as a specific case, the Jeffrey model is considered as an extension of the widely used Newtonian fluid model. In recent researchers during the past (Some recent studies dealing with the Jeffrey fluid [1-4] and several refs. therein).Jeffrey fluid is not just a basic theoretical concept, but this is also used to solve a variety of practical difficulties, such as clay rotational motion and heart vessel pumping. Also, many scientists and researchers looked at how porosity and magnetic fields affected flow behavior in many forms of Jeffrey fluid. Recently, this model of fluid has prompted dynamic discussion (Some of the studies can be observed in [5-8]) investigated the melting effects on stagnation point flow of a Jeffrey fluid in the presence of magnetic field. Akbar, N., Z.H. Khan, and S. Nadeem [9] described , Influence of magnetic field and slip on Jeffrey fluid in a ciliated symmetric channel with metachronal wave pattern. Bhatti, M. and M.A. Abbas [10] investigated the Simultaneous effects of slip and MHD on peristaltic blood flow of Jeffrey fluid model through a porous medium. Sandeep, N. and C. Sulochana [11] have analyzed the Momentum and heat transfer behaviour of Jeffrey, Maxwell and Oldroyd-B nanofluids past a stretching surface with non-uniform heat source/sink. Sandeep et al. [12] studied the Stagnation-point flow of a

* Corresponding author..*E-mail address:* murali.maths81@gmail.com

Jeffrey nanofluid over a stretching surface with induced magnetic field and chemical reaction by similarity transformation.Hayat, T, et al. [13] examined the Three-dimensional flow of Jeffrey nanofluid with a new mass flux condition used by Homotopy analysis method. Soon after on, Shehzad, S.A., et al. [14], Hayat, T., M. Imtiaz, and A. Alsaedi. [15], Dalir, N., M. Dehsara, and S.S. Nourazar [16] investigated a magnetic field effect on the flow of Jeffrey nanofluid in various aspects.

The research regarding interaction between fluid conductors of electricity and magnetic field are concerned with Magnetohydrodynamics. Exact examples of such liquids comprise salt water, liquid metals, plasmas etc. significance and complexity to this interaction between the field and the fluid motion. Reddy M.G., Reddy N.B. [17], proposed, Radiation and mass transfer effects on unsteady MHD free convection flow past a vertical porous plate with viscous dissipation.MHD mixed convection nanofluid flow and heat transfer over an inclined cylinder due to velocity and thermal slip effects are computed by Dhanai, R., P. Rana [18]. Sheikholeslami, M. and D. Ganji [19] examined Nanofluid hydrothermal behavior in existence of Lorentz forces over Joule heating effect. Magnetohydrodynamic (MHD) nonlinear convective flow of Walters-B nanofluid over a nonlinear stretching sheet with variable thickness is scrutinized by Hayat, T., et al. [20]. Waqas, M., et al. [21] formulated micropolar, Carreau and Williamson liquids flow subject to Joule heating. Magnetohydrodynamic (MHD) stratified bioconvective flow of nanofluid due to gyrotactic microorganisms are presented by Alsaedi, A., et al. [22]. Khan, M.I., et al. [23], Qayyum, S., T. Hayat, [24] addressed chemically reacting stretchable flow of magneto third-grade nanoliquid. Kar, M., et al. [25] examined the heat and mass transfer effects on a dissipative and radiative viscoelastic magnetohydrodynamic (MHD) flow over a stretching porous sheet. Basiri Parsa, A., M. Rashidi, and T. Hayat, [26] described the MHD boundary-layer flow over a stretching surface with internal heat generation or absorption. Gupta, P. and A. Gupta [27] have investigated heat and mass transfer in hydrodynamic fluid flow over an isothermalstretching sheet with suction/blowing effects.Devi, S.A., K. Shailendhra, and P. Hemamalini study's [28, 29] focused on Pulsated convective MHD flow with Hall current, heat source and viscous dissipation along a vertical porous plate. The effects of heat and mass transport on an unstable over an infinite vertical plate, hydromagnetic free convection is imbedded in a porous material with heat absorption were examined by Murali, G., A. Paul, and N. Babu [30]. Takhar, H.l.et al. [31, 32], Hall effects on heat and mass transfer flow with variable suction and heat generation. Ahmed, N. and U. Das [33], proposed studied the Convective MHD oscillatory flow past a uniformly moving infinite vertical plate.Caisson fluid performance on natural convective dissipative couette flow past an infinite vertically inclined plate filled in porous medium with heat transfer, mhd and hall current effects. Examined by Babu, N., G. Murali, and S. Bhati [34]. Thermo-Mechanical Vibration embedded in an elastic mediums presented byMohammadi, M., et al. [35-75] investigated Primary and secondary resonance analysis of FG/lipid nanoplate with considering porosity distribution based on a nonlinear elastic medium.

The objective of this study is to look into how a heat source and viscous dissipation affect the flow of the Jeffrey current in a conductor's boundary layer on a vertical plate at high temperatures. Events include things like mass transfers, heat, and magnetic fields. The finite element approach is used to present and solve mathematically Jeffrey's fluid flow model. Effects of each physical parameter are shown and described. A comparative study is also presented the limiting cases and excellent agreement is found. Mathematical study regarding problem formulation is presented in Section 2. Sections 3 and 4 comprise the method of solution and code verification respectively. Discussion related to plots is presented in Section 5. Section 6 lists the main observations.

3.Mathematical Formulation

In this study, we consider the convective motion of a viscous, incompressible, electrically conducting flow of a Jeffrey fluid past a uniformly moving porous plate, with the effects of Hall current and viscous dissipation. Here we assume

(i). The plate is subjected to variable suction velocity;

(ii). The free stream velocity of the fluid oscillates around a constant mean value;

(iii). Except for density, all fluid characteristics remain constant in the buoyancy term (Boussinesq approximation).

(iv). The magnetic dissipation term in the energy equation is negligible;

(v). The low magnetic Reynold number is taken so that the induced magnetic field is negligible.

It uses the Cartesian coordinate system (x', y', z'). The x-axis is measured along the plate in the upward direction and the y-axis is measured normal to the plate in the outward direction. All values are independent of x', with the exception of pressure p'. Within the y'-direction, a magnetic field of constant Bo magnitude is applied. The flow becomes 3-dimensional as the Hall current generates a force in the z'- direction, which results in a cross current in

that direction. The geometry of the problem is shown in Figure 1.
Let (u', v', w') being the velocity's component along the coordinate axes and v_o be the steady suction velocity, therefore section velocity is calculated $v' = v'_o\left(1+\varepsilon e^{(i\omega' t')}\right)$, here 1>>$\varepsilon$. The Cauchy stress tensor $\bar{S}$ for non-Newtonian Jeffreys fluids [29] The Cauchy stress tensor has the below form:

$$S = \frac{\mu}{1+\lambda}\left(\dot{\lambda}+\lambda_1\ddot{\lambda}\right) \tag{1}$$

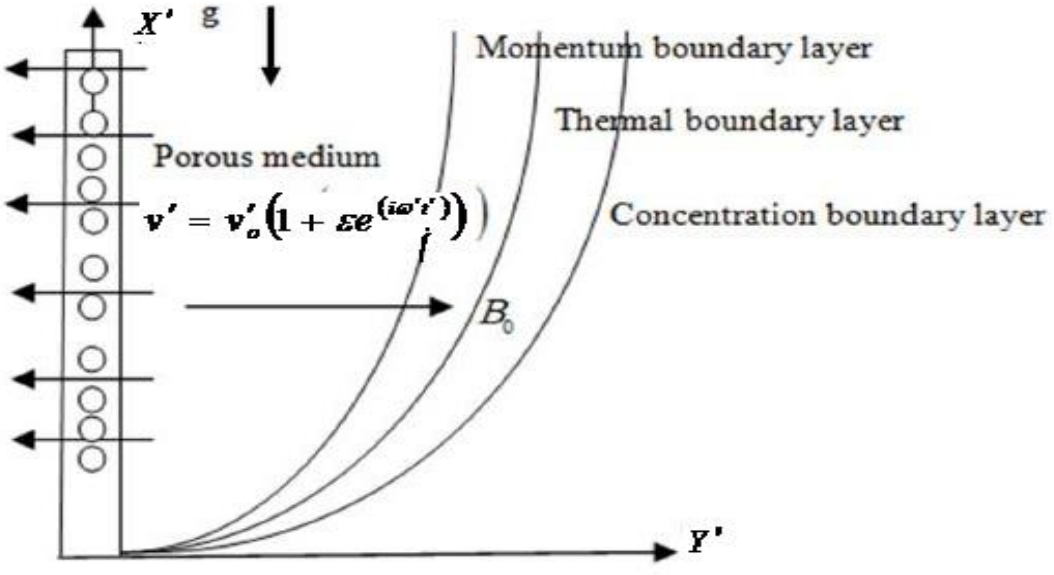

Figure 1. The geometry of the problem.

Here μ is the dynamic viscosity, λ_1 which is the delay relaxation time ratio, and the dot above the number represents the time derivative of the material, λ which is the shear rate. For modelling the effects of retardation and relaxation that take place in a nonNewtonian polymer flow, model provides an elegant formulation. Following is a definition of the shear rate and shear rate gradient in terms of the velocity vector $\bar{V}$:

where $\dot{\lambda} = \nabla\bar{V} + \left(\nabla\bar{V}\right)^T$ (2)

and $\ddot{\lambda} = \frac{d}{dt}\left(\dot{\lambda}\right) + \dot{\lambda}\left(\bar{V}.\nabla\right)$ (3)

The basic physical governing equation for this problem is given in ([28]).

Continuity Equation.:

$$\frac{\partial v'}{\partial y'} = 0 \tag{4}$$

Momentum Equation.:

$$\frac{\partial u'}{\partial t'} + \frac{\partial u'}{\partial y'}v' = \frac{\partial U'}{\partial t'} + \nu\left(\frac{1}{1+\gamma}\right)\frac{\partial^2 u'}{\partial y'^2} + \left(T'-T'_\infty\right)g\beta + \frac{\sigma\mu_e^2 B_o^2}{\rho\left(1+m^2\right)}\left(mw'+u'-U'\right) \tag{5}$$

$$\frac{\partial w'}{\partial t'} + \frac{\partial w'}{\partial y'}v' = \frac{\partial^2 w'}{\partial y'^2}\nu - \left(mu'-mU'-w'\right)\frac{\sigma\mu_e^2 B_o^2}{\rho\left(1+m^2\right)} \tag{6}$$

Equation of Conservation of Energy.:

$$\frac{\partial T'}{\partial t'}+\frac{\partial T'}{\partial y'}v'=\left(\frac{\partial^2 T'}{\partial y'^2}\right)\frac{\kappa}{\rho C_p}+\frac{\nu}{C_p}\left[\left(\frac{\partial u'}{\partial y'}\right)^2+\left(\frac{\partial w'}{\partial y'}\right)^2\right]+\left(T'_\infty-T'\right)Q \tag{7}$$

Here using the formula $U'=U'_o\left(1+\varepsilon e^{(i\omega' t')}\right)$ to get the free stream U' velocity, where U_o' stands for mean stream velocity.

The equivalent boundary conditions ([28]) are

$$\left.\begin{aligned} &t'\le 0: u'=0,\ w'=0,\ T'=T'_\infty\ \forall\ y' \\ &t'>0:\begin{cases} at\ y'=0 \quad u'=V',\ w'=0,\ T'=T'_w \\ as\ y'\to\infty \quad u'=U'(t'),\ w'\to 0,\ T'\to T'_\infty \end{cases} \end{aligned}\right\} \tag{8}$$

Equation (4.) it means that, $v' = v'(t')$. In a thin thermal boundary layer $\frac{\partial v'}{\partial y'}$ is extremely tinythus that can replace $v'=v'_o\left(1+\varepsilon e^{(i\omega' t')}\right)$,$1>>\varepsilon$.

To make the system dimensionless, the following non-dimensional quantities were established.

$$\left.\begin{aligned} &y=\frac{v'_o y'}{\nu},t=\frac{v'^2_o t'}{4\nu},\omega=\frac{4\omega'\nu}{v'^2_o},u=\frac{u'}{U'_o},w=\frac{w'}{U'_o},V=\frac{V'}{U'_o}, \\ &U=\frac{U'}{U'_o},\theta=\frac{T'-T'_\infty}{T'_w-T'_\infty},\mathrm{Pr}=\frac{C_p\nu\rho}{\kappa},Gr=\frac{\left(T'_w-T'_\infty\right)\nu g\beta}{U'_o v'^2_o},S=\frac{\nu^2 Q}{\kappa v'^2_o}, \\ &M^2=\frac{\nu\sigma\mu_e B_o^2}{\rho v'^2_o},\ Ec=\frac{U'^2_o}{C_p\left(T'_w-T'_\infty\right)} \end{aligned}\right\} \tag{9}$$

The coupled partial differential equations that follow from substituting the above relations (9) into equations (5) through (7) are

$$\frac{1}{4}\frac{\partial u}{\partial t}-\left(1+\varepsilon\varepsilon xp(i\omega t)\right)\frac{\partial u}{\partial y}=\left(\frac{1}{1+\gamma}\right)\frac{\partial^2 u}{\partial y^2}+Gr\theta+\frac{1}{4}\frac{\partial U}{\partial t}+\frac{M^2}{m^2+1}\left(mw-u-U\right) \tag{10}$$

$$\frac{1}{4}\frac{\partial w}{\partial t}-\left(1+\varepsilon\varepsilon xp(i\omega t)\right)\frac{\partial w}{\partial y}=\frac{\partial^2 w}{\partial y^2}+\frac{M^2}{1+m^2}\left(mu-w-mU\right) \tag{11}$$

$$\frac{1}{4}\frac{\partial \theta}{\partial t}-\left(1+\varepsilon\varepsilon xp(i\omega t)\right)\frac{\partial \theta}{\partial y}=\frac{1}{\mathrm{Pr}}\frac{\partial^2\theta}{\partial y^2}+Ec\left[\left(\frac{\partial u}{\partial y}\right)^2+\left(\frac{\partial w}{\partial y}\right)^2\right]-S\theta \tag{12}$$

The equivalent boundary conditions are

$$\left.\begin{aligned} &at\ y=0 \quad u=V,\ w=0,\ \theta=1 \\ &as\ y\to\infty\ u=U(t),\ w\to 0,\ \theta\to 0 \end{aligned}\right\} \tag{13}$$

4.Method of Solution

Finite Element Technique:

The finite element procedure (FEM) is a numerical and computer based method of solving a collection of practical engineering problems that happen in different fields such as, in heat transfer, fluid mechanics and many other fields. It is recognized by developers and consumers as one of the most influential numerical analysis tools ever devised to analyze complex problems of engineering. The superiority of the method, its accuracy, simplicity, and computability all make it a widely used apparatus in the engineering modeling and design process. It has been applied to a number of substantial mathematical models, whose differential equations are solved by converting them into a matrix equation. The primary feature of FEM [32] is its ability to describe the geometry or the media of the problem being analyzed with huge flexibility. This is because the discretization of the region of the problem is performed using highly flexible uniform or non-uniform pieces or elements that can easily describe complex shapes. The method essentially consists in assuming the piecewise continuous function for the results and getting the parameters of the functions in a manner that reduces the fault in the solution. The steps occupied in the finite element analysis areas follows.

Step-1: Discretization of the Domain:

The fundamental concept of the FEM is to divide the region of the problem into small connected pieces, called finite elements. The group of elements is called the finite element mesh. These finite elements are associated in a non-overlapping manner, such that they completely cover the entire space of the problem.

Step-2: Invention of the Element Equations:

i) A representative element is secluded from the mesh and the variational formulation of the given problem is created over the typical element.

ii) Over an element, an approximate solution of the variational problem is invented, and by surrogating this in the system, the element equations are generated.

iii) The element matrix, which is also known as stiffness matrix, is erected by using the element interpolation functions.

Step-3: Assembly of the Element Equations:

The algebraic equations so achieved are assembled by imposing the inter element continuity conditions. This yields a large number of mathematical equations known as the global finite element model, which governs the whole domain.

Step-4: Imposition of the Boundary Conditions:

On the accumulated equations, the Dirichlet's and Neumann boundary conditions [13] are imposed.

Step-5: Solution of Assembled Equations:

The assembled equations so obtained can be solved by any of the numerical methods, namely, Gauss elimination technique, LU decomposition technique, and the final matrix equation can be solved by iterative

technique. For computational purposes, the coordinate y varies from 0 to 10, where y_{max} represents infinity external to the momentum, energy and concentration edge layers.

4. 1. 1.Variational formulation

Variation formulation (16)-(18) For a typical linear element $(y_e,\ y_{e+1})$ with two nodes, it is given by

$$\int_{y_e}^{y_{e+1}} w_1\left[\left(\frac{\partial u}{\partial t}\right)-4B\left(\frac{\partial u}{\partial y}\right)-\frac{\partial U}{\partial t}-4\left(\frac{1}{1+\gamma}\right)\frac{\partial^2 u}{\partial y^2}-4(Gr)\theta-\left(\frac{4M^2}{1+m^2}\right)(mw-u-U)\right]dy=0 \tag{14}$$

$$\int_{y_e}^{y_{e+1}} w_2\left[\left(\frac{\partial w}{\partial t}\right)-4B\left(\frac{\partial w}{\partial y}\right)-4\frac{\partial^2 w}{\partial y^2}-\left(\frac{4M^2}{1+m^2}\right)(mu-w-mU)\right]dy=0 \tag{15}$$

$$\int_{y_e}^{y_{e+1}} w_3\left[(\mathrm{Pr})\left(\frac{\partial \theta}{\partial t}\right)-4B(\mathrm{Pr})\left(\frac{\partial \theta}{\partial y}\right)-4\left(\frac{\partial^2 \theta}{\partial y^2}\right)+4S(\mathrm{Pr})\theta-4(Ec)(\mathrm{Pr})\left[\left(\frac{\partial u}{\partial y}\right)^2+\left(\frac{\partial w}{\partial y}\right)^2\right]\right]dy=0 \tag{16}$$

Here $B=1+\varepsilon\exp(i\omega t)$ and $w_1,\ w_2,\ w_3$ are arbitrary test functions, which can viewed whenvariations of $u,\ w$ and θ respectively. The following system of equations results from leaving out the order of integration and nonlinearity:

$$\int_{y_e}^{y_{e+1}}\left[\begin{array}{l}(w_1)\left(\frac{\partial u}{\partial t}\right)-4B\,(w_1)\left(\frac{\partial u}{\partial y}\right)-\frac{\partial U}{\partial t}(w_1)+4\left(\frac{1}{1+\gamma}\right)\left(\frac{\partial w_1}{\partial y}\right)\left(\frac{\partial u}{\partial y}\right)\\ -4(Gr)(w_1)\theta-\left(\frac{4M^2}{1+m^2}\right)(w_1)(mw-u-U)\end{array}\right]dy \tag{17}$$

$$-\left[4(w_1)\left(\frac{1}{1+\gamma}\right)\left(\frac{\partial u}{\partial y}\right)\right]_{y_e}^{y_{e+1}}=0$$

$$\int_{y_e}^{y_{e+1}}\left[(w_2)\left(\frac{\partial w}{\partial t}\right)-4B\,(w_2)\left(\frac{\partial w}{\partial y}\right)+4\left(\frac{\partial w_2}{\partial y}\right)\left(\frac{\partial u}{\partial y}\right)-\left(\frac{4M^2}{1+m^2}\right)(w_2)(mu-w-mU)\right]dy \tag{18}$$

$$-\left[4(w_2)\left(\frac{\partial w}{\partial y}\right)\right]_{y_e}^{y_{e+1}}=0$$

$$\int_{y_e}^{y_{e+1}}\left[(w_3)(\mathrm{Pr})\left(\frac{\partial \theta}{\partial t}\right)-4B(\mathrm{Pr})(w_3)\left(\frac{\partial \theta}{\partial y}\right)+4\left(\frac{\partial w_3}{\partial y}\right)\left(\frac{\partial \theta}{\partial y}\right)+4(\mathrm{Pr})S(w_3)\theta-4(Ec)(\mathrm{Pr})\left[\left(\frac{\partial u}{\partial y}\right)\left(\frac{\partial \bar{u}}{\partial y}\right)+\left(\frac{\partial w}{\partial y}\right)\left(\frac{\partial \bar{w}}{\partial y}\right)\right]\right]dy$$

$$-\left[4(w_2)\left(\frac{\partial \theta}{\partial y}\right)\right]_{y_e}^{y_{e+1}}=0 \tag{19}$$

4.1.2. Finite Element formulation:

Equations (17) through (19) can be used to derive a finite element model by replace with the finite element approximation of the form.

$$u = \sum_{j=1}^{2} u_j^e \psi_j^e,\ w = \sum_{j=1}^{2} w_j^e \psi_j^e,\ \theta = \sum_{j=1}^{2} \theta_j^e \psi_j^e \tag{20}$$

among $w_1 = w_2 = w_3 = \psi_j^e\ (i = 1, 2)$, Here u_j^e, w_j^e and θ_j^e be the velocity, temperature, and concentration on nodal points of a symbolic element, respectively, on j^{th} node of emblematic e^{th} element $(y_e,\ y_{e+1})$ and ψ_i^e be the shape function of that element $(y_e,\ y_{e+1})$, and beassumed to be:

$$\psi_1^e = \frac{y_{e+1} - y}{y_{e+1} - y_e} \text{ and } \psi_2^e = \frac{y - y_e}{y_{e+1} - y_e},\ y_e \le y \le y_{e+1} \tag{21}$$

The finite element model of the e^{th} element equation hence formed is given here

$$\begin{bmatrix} [K^{11}] & [K^{12}] & [K^{13}] \\ [K^{21}] & [K^{22}] & [K^{23}] \\ [K^{31}] & [K^{32}] & [K^{33}] \end{bmatrix} \begin{bmatrix} \{u^e\} \\ \{w^e\} \\ \{\theta^e\} \end{bmatrix} + \begin{bmatrix} [M^{11}] & [M^{12}] & [M^{13}] \\ [M^{21}] & [M^{22}] & [M^{23}] \\ [M^{31}] & [M^{32}] & [M^{33}] \end{bmatrix} \begin{bmatrix} \{u'^e\} \\ \{w'^e\} \\ \{\theta'^e\} \end{bmatrix} = \begin{bmatrix} \{b^{1e}\} \\ \{b^{2e}\} \\ \{b^{3e}\} \end{bmatrix} \tag{22}$$

Here $\{[K^{mn}], [M^{mn}]\}$ and $\{\{u^e\}, \{\theta^e\}, \{\phi^e\}, \{u'^e\}, \{\theta'^e\}, \{\phi'^e\} \text{ and } \{b^{me}\}\}(m, n = 1, 2, 3)$ are each a set of ordered matrices 2×2 and 2×1 respectively.. These matrices are defined as:

$$K_{ij}^{11} = -4B \int_{y_e}^{y_{e+1}} \left[(\psi_i^e) \left(\frac{\partial \psi_j^e}{\partial y} \right) \right] dy + 4 \left(\frac{1}{1+\gamma} \right) \int_{y_e}^{y_{e+1}} \left[\left(\frac{\partial \psi_i^e}{\partial y} \right) \left(\frac{\partial \psi_j^e}{\partial y} \right) \right] dy,$$

$$M_{ij}^{11} = M_{ij}^{22} = M_{ij}^{33} = \int_{y_e}^{y_{e+1}} (\psi_i^e)(\psi_j^e) dy,\ M_{ij}^{12} = M_{ij}^{13} = 0,$$

$$K_{ij}^{12} = -\left(\frac{4M^2}{1+m^2} \right) m \int_{y_e}^{y_{e+1}} [(\psi_i^e)(\psi_j^e)] dy + \left(\frac{4M^2}{1+m^2} \right) \int_{y_e}^{y_{e+1}} [(\psi_i^e)(\psi_j^e)] dy + \left(\frac{4M^2 U}{1+m^2} \right) \int_{y_e}^{y_{e+1}} [(\psi_j^e)] dy - \left(\frac{\partial U}{\partial t} \right) \int_{y_e}^{y_{e+1}} [\psi_i^e] dy,$$

$$K_{ij}^{13} = -[Gr] \int_{y_e}^{y_{e+1}} (\psi_i^e)(\psi_j^e) dy,$$

$$M_{ij}^{31} = M_{ij}^{32} = 0, \qquad K_{ij}^{21} = 0, \qquad K_{ij}^{31} = 0, \qquad M_{ij}^{21} = M_{ij}^{23} = 0,$$

$$K_{ij}^{22} = -4B \int_{y_e}^{y_{e+1}} \left[(\psi_i^e) \left(\frac{\partial \psi_j^e}{\partial y} \right) \right] dy + 4 \int_{y_e}^{y_{e+1}} \left[\left(\frac{\partial \psi_i^e}{\partial y} \right) \left(\frac{\partial \psi_j^e}{\partial y} \right) \right] dy,$$

$$K_{ij}^{23} = -\left(\frac{4M^2}{1+m^2} \right) m \int_{y_e}^{y_{e+1}} [(\psi_i^e)(\psi_j^e)] dy + \left(\frac{4M^2}{1+m^2} \right) \int_{y_e}^{y_{e+1}} [(\psi_i^e)(\psi_j^e)] dy + \left(\frac{4M^2 mU}{1+m^2} \right) \int_{y_e}^{y_{e+1}} [(\psi_j^e)] dy,$$

$$K_{ij}^{32} = -4B(\Pr)\int_{y_e}^{y_{e+1}}\left[\left(\psi_i^e\left(\frac{\partial\psi_j^e}{\partial y}\right)\right]dy + 4\int_{y_e}^{y_{e+1}}\left[\left(\frac{\partial\psi_i^e}{\partial y}\right)\left(\frac{\partial\psi_j^e}{\partial y}\right)\right]dy,$$

$$K_{ij}^{33} = 4(\Pr)S\int_{y_e}^{y_{e+1}}\left[\psi_i^e\right]dy - 8(\Pr)(Ec)\int_{y_e}^{y_{e+1}}\left[\left(\frac{\partial\psi_i^e}{\partial y}\right)\left(\frac{\partial\psi_j^e}{\partial y}\right)\right](\psi_i^e)dy, \qquad b_i^{1e} = \left[4\left(\frac{1}{1+\gamma}\right)\left(\psi_i^e\left(\frac{\partial\psi_j^e}{\partial y}\right)\right]_{y_e}^{y_{e+1}},\right.$$

$$b_i^{2e} = \left[4\left(\psi_i^e\left(\frac{\partial\psi_j^e}{\partial y}\right)\right]_{y_e}^{y_{e+1}}, \; b_i^{3e} = \left[4(\Pr)\left(\psi_i^e\left(\frac{\partial\psi_j^e}{\partial y}\right)\right]_{y_e}^{y_{e+1}}\right.$$

Linear components are comparable to tin in 1-dimensional space. The area of the stream is divided into 11,000 equal-sized square cells. The total domain consists of his 21001 nodes because each element has 3 nodes. Each node needs to evaluate four functions. As a result, after merging the finite element equations, we obtain an 8100 equation nonlinear system.so, you should develop an iterative scheme within your solution. When the boundary conditions are satisfied, we obtain a system of equations that is mathematically solved using Gaussian elimination with an accuracy of 0.00001. The relative dissimilarity between this iteration and the preceding iteration it is employed as a convergence criterion.

When these discrepancies are as accurate as desired, The iterative process is deemed to have ended when the solution has converged.The integral be resolved using Gaussian quadrature. His computer's MATLAB function is running an algorithmic computer script. Achieving good convergence for each outcome.

4.1.3. Program Code Validation:

i. In conclusion, Fig. 2 shows a qualitative comparison of these results in the absence of Jeffrey fluid within the puIlished results of Anjali Devi et al. [28.].The current results for some flow parameters differ significantly in both qualitative and quantitative terms.

ii. At first, the numerical results are similar to Takhar et al. [32] when viscous dissipation is ignored, as personalizedGrashofGc = 0 and Schmidt number Sc = 0.

iii. Furthermore, by ignoring Hall effect,be recoverable from our numerical results, and the conclusions of Ahmed and Das [33.],and such a similarity is probableby profiles with m = 0.

5.Results and Discussion:

To examine the results, numerical calculationsbemade for the variations of the governing parameters,for exampleGr, M^2, Pr, Ec, S, m, γ. The following default parameter values are used in the calculations in this study.:Gr = 2.0, m = 1.0; S = 1.0; M^2 = 1.0; Pr = 0.71; Ec = 0.001; γ = 1.0; and V= 1.0.The following default parameter values are used in the calculations in this study.

The influence The influence of primary velocity profiles u for different values of Grashof number for heat transfer Gr, and Magnetic field parameter M^2 in Fig. 3. It is observed that the dimensionless primary velocity

profiles increase and decreases with *Gr* and M^2, respectively. This is due to the fact that the introduction of a transverse magnetic field, normal to the flow direction, has a tendency to create the drag known as the Lorentz force which tends to resist the flow. It is revealed from Fig. 5 that, secondary fluid velocity w increases on increasing *Gr* and M^2 throughout the boundary layer region. The Eckert number *Ec* is the ratio of kinetic energy to the thermal energy. When *Ec* is increased, it is seen from Figs. 4 and 6 that both the velocity components *u* and *w* increase, which is physically expected. Further, an increase in Eckert number *Ec* also increases the temperature as can be seen from Fig. 4. This is because convection dominates over conduction in such a case. Figs. 3 and 4 demonstrate the effect of Hall current on the primary velocity *u* and secondary velocity w respectively. It is perceived from Figs. 3 and 5 that, the primary velocity *u* decreases on increasing *m* throughout the boundary layer region whereas secondary velocity w increases on increasing m throughout the boundary layer region. This implies that, Hall current tends to accelerate secondary fluid velocity throughout the boundary layer region which is consistent with the fact that Hall current induces secondary flow in the flow-field whereas it has a reverse effect on primary fluid velocity throughout the boundary layer region. Fig. 3 is made to see the variation of primary velocity profiles *u* for different values of Jeffrey fluid parameter. As depicted in this figure, the effect of increasing γ lead to enhance the fluid velocity gradually in the right half of the channel. From Figs. 4 and 6, it is clear that the effect of the heat source parameter on the velocity components *u* and *w* is to modify the flow away from the plate so as to decrease them and its effect within the boundary layer is not very significant. Further, is found to decrease temperature uniformly throughout the flow region (Fig. 7). It is obvious from Figs. 4 and 5 that the velocity components u as well as w are reduced by Prandtl number *Pr*. In Fig. 7, it is observed that the temperature decreases with increasing values of Prandtl number. It is also observed that the thermal boundary layer thickness is maximum near the surface of the cone and decreases with increasing distances from the leading edge and finally approaches to zero. It is justified due to the fact that thermal conductivity of fluid decreases with increasing Prandtl number and hence decreases the thermal boundary layer thickness and the temperature profiles. The parameter *V* is the ratio of the velocity of the plate and the mean free stream velocity of the fluid. In general, u increases when *V* is increased and the flow pattern within the boundary layer is significantly modified when *V* is greater than unity (Fig. 3) and this is in good agreement with the no-slip boundary condition of viscous fluids. An increase in temperature and thermal boundary layer thickness is observed for the larger values of Eckert number. Here the increasing values of Eckert number give rise to the temperature difference that leads to higher temperature and thermal boundary layer thickness (see Fig.7).

5.Conclusions

This research work presents free convective magnetohydrodynamic non-newtonian Jeffrey fluid flow with Hall current, heat source and variable suction towards a vertical plate. The governing coupled non-linear partial differential equations of the problem is reduced to linear partial differential equations have been obtained using the finite element method. The primary velocity profiles, secondary velocity profiles and temperature fields are discussed with the help of graphs. The main points of this paper may be summarized and the following characteristics have been observed.

1. As raising Magnetic field parameter, heat source parameter and Prandtl number tends to suppress the fluid primary velocity profiles whereas reverse is true with Grashof number for heat transfer, Eckert number, Jeffrey fluid and Hall parameters.
2. As increasing the magnetic parameter, the Grash of heat transfer number, and the Eckert number produce a quadratic velocity field, while increasing the Prandtl number, the Hall parameter, and the heat source parameter the opposite effect is observed
3. When the values of Prandtl number increase, the temperature field getting down and an increase in Eckert number gives rise to the temperature field.

References

[1] T. Hayat, M. Mustafa, Influence of thermal radiation on the unsteady mixed convection flow of a Jeffrey fluid over a stretching sheet, *Zeitschrift für Naturforschung A*, Vol. 65, No. 8-9, pp. 711-719, 2010.

[2] K. Das, Influence of slip and heat transfer on MHD peristaltic flow of a Jeffrey fluid in an inclined asymmetric porous channel, *Indian Journal of Mathematics*, Vol. 54, No. 1, pp. 19-45, 2012.

[3] M. Qasim, Heat and mass transfer in a Jeffrey fluid over a stretching sheet with heat source/sink, *Alexandria Engineering Journal*, Vol. 52, No. 4, pp. 571-575, 2013.

[4] T. Hayat, N. Ahmad, N. Ali, Effects of an endoscope and magnetic field on the peristalsis involving Jeffrey fluid, *Communications in Nonlinear Science and Numerical Simulation,* Vol. 13, No. 8, pp. 1581-1591, 2008.

[5] S. Shehzad, A. Alsaedi, T. Hayat, Influence of thermophoresis and Joule heating on the radiative flow of Jeffrey fluid with mixed convection, *Brazilian Journal of Chemical Engineering,* Vol. 30, pp. 897-908, 2013.

[6] S. Nallapu, G. Radhakrishnamacharya, Jeffrey fluid flow through porous medium in the presence of magnetic field in narrow tubes, *International Journal of Engineering Mathematics,* Vol. 2014, 2014.

[7] V. Ramachandra Prasad, S. Abdul Gaffar, E. Keshava Reddy, O. Anwar Bég, S. Krishnaiah, A mathematical study for laminar boundary-layer flow, heat, and mass transfer of a Jeffrey non-Newtonian fluid past a vertical porous plate, *Heat Transfer—Asian Research,* Vol. 44, No. 3, pp. 189-210, 2015.

[8] K. Das, L. Zheng, Melting effects on the stagnation point flow of a Jeffrey fluid in the presence of magnetic field, *Heat Transfer Research,* Vol. 44, No. 6, 2013.

[9] N. Akbar, Z. H. Khan, S. Nadeem, Influence of magnetic field and slip on Jeffrey fluid in a ciliated symmetric channel with metachronal wave pattern, *Journal of Applied Fluid Mechanics,* Vol. 9, No. 2, pp. 565-572, 2016.

[10] M. Bhatti, M. A. Abbas, Simultaneous effects of slip and MHD on peristaltic blood flow of Jeffrey fluid model through a porous medium, *Alexandria Engineering Journal,* Vol. 55, No. 2, pp. 1017-1023, 2016.

[11] N. Sandeep, C. Sulochana, Momentum and heat transfer behaviour of Jeffrey, Maxwell and Oldroyd-B nanofluids past a stretching surface with non-uniform heat source/sink, *Ain Shams Engineering Journal,* Vol. 9, No. 4, pp. 517-524, 2018.

[12] N. Sandeep, C. Sulochana, I. L. Animasaun, Stagnation-point flow of a Jeffrey nanofluid over a stretching surface with induced magnetic field and chemical reaction, in *Proceeding of,* Trans Tech Publ, pp. 93-111.

[13] T. Hayat, T. Muhammad, S. A. Shehzad, A. Alsaedi, Three-dimensional flow of Jeffrey nanofluid with a new mass flux condition, *Journal of Aerospace Engineering,* Vol. 29, No. 2, pp. 04015054, 2016.

[14] S. A. Shehzad, T. Hayat, A. Alsaedi, M. A. Obid, Nonlinear thermal radiation in three-dimensional flow of Jeffrey nanofluid: a model for solar energy, *Applied Mathematics and Computation,* Vol. 248, pp. 273-286, 2014.

[15] T. Hayat, M. Imtiaz, A. Alsaedi, Magnetohydrodynamic stagnation point flow of a Jeffrey nanofluid with Newtonian heating, *Journal of aerospace engineering,* Vol. 29, No. 3, pp. 04015063, 2016.

[16] N. Dalir, M. Dehsara, S. S. Nourazar, Entropy analysis for magnetohydrodynamic flow and heat transfer of a Jeffrey nanofluid over a stretching sheet, *Energy,* Vol. 79, pp. 351-362, 2015.

[17] R. V. Prasad, B. N. Reddy, Radiation and mass transfer effects on an unsteady MHD free convection flow past a heated vertical plate in a porous medium with viscous dissipation, *Theoretical and Applied Mechanics,* Vol. 34, No. 2, pp. 135-160, 2007.

[18] R. Dhanai, P. Rana, L. Kumar, MHD mixed convection nanofluid flow and heat transfer over an inclined cylinder due to velocity and thermal slip effects: Buongiorno's model, *Powder Technology,* Vol. 288, pp. 140-150, 2016.

[19] M. Sheikholeslami, D. Ganji, Nanofluid hydrothermal behavior in existence of Lorentz forces considering Joule heating effect, *Journal of Molecular Liquids,* Vol. 224, pp. 526-537, 2016.

[20] T. Hayat, S. Qayyum, A. Alsaedi, B. Ahmad, Magnetohydrodynamic (MHD) nonlinear convective flow of Walters-B nanofluid over a nonlinear stretching sheet with variable thickness, *International Journal of Heat and Mass Transfer,* Vol. 110, pp. 506-514, 2017.

[21] M. Waqas, M. Farooq, M. I. Khan, A. Alsaedi, T. Hayat, T. Yasmeen, Magnetohydrodynamic (MHD) mixed convection flow of micropolar liquid due to nonlinear stretched sheet with convective condition, *International Journal of Heat and Mass Transfer,* Vol. 102, pp. 766-772, 2016.

[22] A. Alsaedi, M. I. Khan, M. Farooq, N. Gull, T. Hayat, Magnetohydrodynamic (MHD) stratified bioconvective flow of nanofluid due to gyrotactic microorganisms, *Advanced Powder Technology,* Vol. 28, No. 1, pp. 288-298, 2017.

[23] M. I. Khan, M. Waqas, T. Hayat, M. I. Khan, A. Alsaedi, Behavior of stratification phenomenon in flow of Maxwell nanomaterial with motile gyrotactic microorganisms in the presence of magnetic field, *International Journal of Mechanical Sciences,* Vol. 131, pp. 426-434, 2017.

[24] S. Qayyum, T. Hayat, A. Alsaedi, Chemical reaction and heat generation/absorption aspects in MHD nonlinear convective flow of third grade nanofluid over a nonlinear stretching sheet with variable thickness, *Results in physics,* Vol. 7, pp. 2752-2761, 2017.

[25] M. Kar, S. Sahoo, P. Rath, G. Dash, Heat and mass transfer effects on a dissipative and radiative visco-elastic MHD flow over a stretching porous sheet, *Arabian Journal for Science and Engineering*, Vol. 39, pp. 3393-3401, 2014.

[26] A. Basiri Parsa, M. Rashidi, T. Hayat, MHD boundary-layer flow over a stretching surface with internal heat generation or absorption, *Heat Transfer—Asian Research*, Vol. 42, No. 6, pp. 500-514, 2013.

[27] P. Gupta, A. Gupta, Heat and mass transfer on a stretching sheet with suction or blowing, *The Canadian journal of chemical engineering*, Vol. 55, No. 6, pp. 744-746, 1977.

[28] S. A. Devi, S. Karthikeyan, P. Hemamalini, Pulsated convective MHD flow with Hall current, heat source and viscous dissipation along a vertical porous plate, *Education*, Vol. 2002, 1991.

[29] P. Sturdza, 2004, *An aerodynamic design method for supersonic natural laminar flow aircraft*, stanford university,

[30] G. Murali, A. Paul, N. Babu, Heat and mass transfer effects on an unsteady hydromagnetic free convective flow over an infinite vertical plate embedded in a porous medium with heat absorption, *Int. J. Open Problems Compt. Math*, Vol. 8, No. 1, 2015.

[31] H. Takhar, P. Ram, S. Singh, Hall effects on heat and mass transfer flow with variable suction and heat generation, *Astrophysics and space science*, Vol. 191, pp. 101-106, 1992.

[32] J. N. Reddy, 2019, *Introduction to the finite element method*, McGraw-Hill Education,

[33] N. Ahmed, U. Das, Convective MHD oscillatory flow past a uniformly moving infinite vertical plate, *Defence Science Journal*, Vol. 42, No. 1, pp. 53, 1992.

[34] N. BABU, G. MURALI, S. BHATI, Casson fluid performance on natural convective dissipative couette flow past an infinite vertically inclined plate filled in porous medium with heat transfer, mhd and hall current effects, *International Journal of Pharmaceutical Research*, Vol. 10, No. 4, 2018.

[35] M. Mohammadi, A. Farajpour, A. Moradi, M. Hosseini, Vibration analysis of the rotating multilayer piezoelectric Timoshenko nanobeam, *Engineering Analysis with Boundary Elements*, Vol. 145, pp. 117-131, 2022.

[36] M. Mohammadi, A. Rastgoo, Primary and secondary resonance analysis of FG/lipid nanoplate with considering porosity distribution based on a nonlinear elastic medium, *Mechanics of Advanced Materials and Structures*, Vol. 27, No. 20, pp. 1709-1730, 2020.

[37] M. Mohammadi, M. Hosseini, M. Shishesaz, A. Hadi, A. Rastgoo, Primary and secondary resonance analysis of porous functionally graded nanobeam resting on a nonlinear foundation subjected to mechanical and electrical loads, *European Journal of Mechanics-A/Solids*, Vol. 77, pp. 103793, 2019.

[38] M. Mohammadi, A. Rastgoo, Nonlinear vibration analysis of the viscoelastic composite nanoplate with three directionally imperfect porous FG core, *Structural Engineering and Mechanics, An Int'l Journal*, Vol. 69, No. 2, pp. 131-143, 2019.

[39] A. Farajpour, A. Rastgoo, M. Mohammadi, Vibration, buckling and smart control of microtubules using piezoelectric nanoshells under electric voltage in thermal environment, *Physica B: Condensed Matter*, Vol. 509, pp. 100-114, 2017.

[40] A. Farajpour, M. H. Yazdi, A. Rastgoo, M. Loghmani, M. Mohammadi, Nonlocal nonlinear plate model for large amplitude vibration of magneto-electro-elastic nanoplates, *Composite Structures*, Vol. 140, pp. 323-336, 2016.

[41] A. Farajpour, M. H. Yazdi, A. Rastgoo, M. Mohammadi, A higher-order nonlocal strain gradient plate model for buckling of orthotropic nanoplates in thermal environment, *Acta Mechanica*, Vol. 227, pp. 1849-1867, 2016.

[42] M. Mohammadi, M. Safarabadi, A. Rastgoo, A. Farajpour, Hygro-mechanical vibration analysis of a rotating viscoelastic nanobeam embedded in a visco-Pasternak elastic medium and in a nonlinear thermal environment, *Acta Mechanica*, Vol. 227, pp. 2207-2232, 2016.

[43] M. R. Farajpour, A. Rastgoo, A. Farajpour, M. Mohammadi, Vibration of piezoelectric nanofilm-based electromechanical sensors via higher-order non-local strain gradient theory, *Micro & Nano Letters*, Vol. 11, No. 6, pp. 302-307, 2016.

[44] M. Baghani, M. Mohammadi, A. Farajpour, Dynamic and stability analysis of the rotating nanobeam in a nonuniform magnetic field considering the surface energy, *International Journal of Applied Mechanics*, Vol. 8, No. 04, pp. 1650048, 2016.

[45] M. Goodarzi, M. Mohammadi, M. Khooran, F. Saadi, Thermo-mechanical vibration analysis of FG circular and annular nanoplate based on the visco-pasternak foundation, *Journal of Solid Mechanics*, Vol. 8, No. 4, pp. 788-805, 2016.

[46] H. Asemi, S. Asemi, A. Farajpour, M. Mohammadi, Nanoscale mass detection based on vibrating piezoelectric ultrathin films under thermo-electro-mechanical loads, *Physica E: Low-dimensional Systems and Nanostructures*, Vol. 68, pp. 112-122, 2015.

[47] M. Safarabadi, M. Mohammadi, A. Farajpour, M. Goodarzi, Effect of surface energy on the vibration analysis of rotating nanobeam, 2015.

[48] M. Goodarzi, M. Mohammadi, A. Gharib, Techno-Economic Analysis of Solar Energy for Cathodic Protection of Oil and Gas Buried Pipelines in Southwestern of Iran, in *Proceeding of*, https://publications.waset.org/abstracts/33008/techno-economic-analysis-of …, pp.

[49] M. Mohammadi, A. A. Nekounam, M. Amiri, The vibration analysis of the composite natural gas pipelines in the nonlinear thermal and humidity environment, in *Proceeding of*, https://civilica.com/doc/540946/, pp.

[50] M. Goodarzi, M. Mohammadi, M. Rezaee, Technical Feasibility Analysis of PV Water Pumping System in Khuzestan Province-Iran, in *Proceeding of*, https://publications.waset.org/abstracts/18930/technical-feasibility …, pp.

[51] M. Mohammadi, A. Farajpour, A. Moradi, M. Ghayour, Shear buckling of orthotropic rectangular graphene sheet embedded in an elastic medium in thermal environment, *Composites Part B: Engineering*, Vol. 56, pp. 629-637, 2014.

[52] M. Mohammadi, A. Moradi, M. Ghayour, A. Farajpour, Exact solution for thermo-mechanical vibration of orthotropic mono-layer graphene sheet embedded in an elastic medium, *Latin American Journal of Solids and Structures*, Vol. 11, pp. 437-458, 2014.

[53] M. Mohammadi, A. Farajpour, M. Goodarzi, F. Dinari, Thermo-mechanical vibration analysis of annular and circular graphene sheet embedded in an elastic medium, *Latin American Journal of Solids and Structures*, Vol. 11, pp. 659-682, 2014.

[54] M. Mohammadi, A. Farajpour, M. Goodarzi, Numerical study of the effect of shear in-plane load on the vibration analysis of graphene sheet embedded in an elastic medium, *Computational Materials Science*, Vol. 82, pp. 510-520, 2014.

[55] A. Farajpour, A. Rastgoo, M. Mohammadi, Surface effects on the mechanical characteristics of microtubule networks in living cells, *Mechanics Research Communications*, Vol. 57, pp. 18-26, 2014.

[56] S. R. Asemi, M. Mohammadi, A. Farajpour, A study on the nonlinear stability of orthotropic single-layered graphene sheet based on nonlocal elasticity theory, *Latin American Journal of Solids and Structures*, Vol. 11, pp. 1541-1546, 2014.

[57] M. Goodarzi, M. Mohammadi, A. Farajpour, M. Khooran, Investigation of the effect of pre-stressed on vibration frequency of rectangular nanoplate based on a visco-Pasternak foundation, 2014.

[58] S. Asemi, A. Farajpour, H. Asemi, M. Mohammadi, Influence of initial stress on the vibration of double-piezoelectric-nanoplate systems with various boundary conditions using DQM, *Physica E: Low-dimensional Systems and Nanostructures*, Vol. 63, pp. 169-179, 2014.

[59] S. Asemi, A. Farajpour, M. Mohammadi, Nonlinear vibration analysis of piezoelectric nanoelectromechanical resonators based on nonlocal elasticity theory, *Composite Structures*, Vol. 116, pp. 703-712, 2014.

[60] M. Mohammadi, M. Ghayour, A. Farajpour, Free transverse vibration analysis of circular and annular graphene sheets with various boundary conditions using the nonlocal continuum plate model, *Composites Part B: Engineering*, Vol. 45, No. 1, pp. 32-42, 2013.

[61] M. Mohammadi, M. Goodarzi, M. Ghayour, A. Farajpour, Influence of in-plane pre-load on the vibration frequency of circular graphene sheet via nonlocal continuum theory, *Composites Part B: Engineering*, Vol. 51, pp. 121-129, 2013.

[62] M. Mohammadi, A. Farajpour, M. Goodarzi, R. Heydarshenas, Levy type solution for nonlocal thermo-mechanical vibration of orthotropic mono-layer graphene sheet embedded in an elastic medium, *Journal of Solid Mechanics*, Vol. 5, No. 2, pp. 116-132, 2013.

[63] M. Mohammadi, A. Farajpour, M. Goodarzi, H. Mohammadi, Temperature Effect on Vibration Analysis of Annular Graphene Sheet Embedded on Visco-Pasternak Foundati, *Journal of Solid Mechanics*, Vol. 5, No. 3, pp. 305-323, 2013.

[64] M. Danesh, A. Farajpour, M. Mohammadi, Axial vibration analysis of a tapered nanorod based on nonlocal elasticity theory and differential quadrature method, *Mechanics Research Communications*, Vol. 39, No. 1, pp. 23-27, 2012.

[65] A. Farajpour, A. Shahidi, M. Mohammadi, M. Mahzoon, Buckling of orthotropic micro/nanoscale plates under linearly varying in-plane load via nonlocal continuum mechanics, *Composite Structures*, Vol. 94, No. 5, pp. 1605-1615, 2012.

[66] M. Mohammadi, M. Goodarzi, M. Ghayour, S. Alivand, Small scale effect on the vibration of orthotropic plates embedded in an elastic medium and under biaxial in-plane pre-load via nonlocal elasticity theory, 2012.

[67] A. Farajpour, M. Mohammadi, A. Shahidi, M. Mahzoon, Axisymmetric buckling of the circular graphene sheets with the nonlocal continuum plate model, *Physica E: Low-dimensional Systems and Nanostructures*, Vol. 43, No. 10, pp. 1820-1825, 2011.

[68] A. Farajpour, M. Danesh, M. Mohammadi, Buckling analysis of variable thickness nanoplates using nonlocal continuum mechanics, *Physica E: Low-dimensional Systems and Nanostructures*, Vol. 44, No. 3, pp. 719-727, 2011.

[69] H. Moosavi, M. Mohammadi, A. Farajpour, S. Shahidi, Vibration analysis of nanorings using nonlocal continuum mechanics and shear deformable ring theory, *Physica E: Low-dimensional Systems and Nanostructures*, Vol. 44, No. 1, pp. 135-140, 2011.

[70] M. Mohammadi, M. Ghayour, A. Farajpour, Analysis of free vibration sector plate based on elastic medium by using new version differential quadrature method, *Journal of solid mechanics in engineering*, Vol. 3, No. 2, pp. 47-56, 2011.

[71] A. Farajpour, M. Mohammadi, M. Ghayour, Shear buckling of rectangular nanoplates embedded in elastic medium based on nonlocal elasticity theory, in *Proceeding of*, www.civilica.com/Paper-ISME19-ISME19_390.html, pp. 390.

[72] M. Mohammadi, A. Farajpour, A. R. Shahidi, Higher order shear deformation theory for the buckling of orthotropic rectangular nanoplates using nonlocal elasticity, in *Proceeding of*, www.civilica.com/Paper-ISME19-ISME19_391.html, pp. 391.

[73] M. Mohammadi, A. Farajpour, A. R. Shahidi, Effects of boundary conditions on the buckling of single-layered graphene sheets based on nonlocal elasticity, in *Proceeding of*, www.civilica.com/Paper-ISME19-ISME19_382.html, pp. 382.

[74] M. Mohammadi, M. Ghayour, A. Farajpour, Using of new version integral differential method to analysis of free vibration orthotropic sector plate based on elastic medium, in *Proceeding of*, www.civilica.com/Paper-ISME19-ISME19_497.html, pp. 497.

[75] M. Mohammadi, A. Farajpour, A. Rastgoo, Coriolis effects on the thermo-mechanical vibration analysis of the rotating multilayer piezoelectric nanobeam, *Acta Mechanica*, Vol. 234, No. 2, pp. 751-774, 2023/02/01, 2023.